

## Nonequilibrium Solidification of Monocrystalline Si Induced by ArF-Excimer-Laser Irradiation

R. Černý<sup>a</sup>, I. Lukes<sup>b</sup>, V. Chab<sup>b</sup> and R. Sasik<sup>b</sup>,

<sup>a</sup>*Faculty of Civil Engineering, Czech Technical University, Thakurova 7, 166 29 Prague 6, Czechoslovakia*

<sup>b</sup>*Institute of Physics, Czechoslovak Academy of Sciences, Na Slovance 2, 180 40 Prague 8, Czechoslovakia*

Keywords : nonequilibrium solidification, excimer laser, mathematical modeling, surface structure, monocrystalline Si

### ABSTRACT

Results of theoretical and experimental study of ArF-excimer-laser-induced recrystallization of monocrystalline Si(100) surface are presented. The theoretical model of laser-induced thermal processes including the density changes due to thermal expansion and phase-changing is introduced. Comparison of calculated data with in situ LEED analysis indicate a significant correlation between laser-induced high solidification velocity and/or undercooling and crystalline structure of the irradiated surfaces.

### INTRODUCTION

Irradiation of semiconductors by a short (nanosecond) laser pulse with energy density above a certain threshold produces fast melting of a thin surface layer followed by its rapid resolidification. Heating and cooling rates are orders of magnitude faster than those achieved by any other treatment; solidification at fast moving liquid-solid interface takes place under conditions far from thermal equilibrium. Zehner (1984) has reported "bulklike" (1 × 1) structure on clean Si(111) surface as result of the ruby-laser irradiation in ultra-high vacuum (UHV). More recently, Kubatova et al. (1989) have prepared (1 × 1) Si(100)

clean surface by ArF-excimer-laser irradiation. They reported the possibility to control reversibly the resulted structure ( $1 \times 1$ ) or ( $2 \times 1$ ) by changing the initial temperature of the irradiated sample. Liu et al. (1979) and Cullis et al. (1982) reported that at velocities above certain value the structural rearrangement at the liquid-solid interface did not proceed, and the amorphous phase was produced. These experimental results indicate nonequilibrium character of the thermal processes involved.

In the last decades, the mostly used approach to theoretical modeling of nonequilibrium thermal processes was the equilibrium model [see eg. Baeri et al.(1979); Wood and Giles (1981)], based on the assumption that introduction of interfacial kinetics is not necessary. However, in many cases the interface motion is so fast, that this assumption is not longer valid, and strong overheating and/or undercooling must be taken into account. There are two basic phenomenological formulations used for the description of nonequilibrium processes; the first one emphasizes thermodynamical concepts [Turnbull (1956); Spaepen and Turnbull (1982)], while the other one, based on the kinetic rate theory, emphasizes molecular kinetics at the solid-liquid interface [Jackson and Chalmers (1956); Jackson (1975)].

Previously published models of the nonequilibrium phase transitions [Wood and Geist (1986)] are based on enthalpy considerations. The position of the phase interface is not treated explicitly but it is derived from the local enthalpy contents in the sample. Recently, Sasik and Cerny (1991) and Cerny et al. (1991) replaced the condition of a local thermodynamic equilibrium at the phase interface with the interface response function and the interface itself treated explicitly as a position of the moving boundary between the solid and liquid phases. In this paper we present a more general model embracing also thermal expansion of both phases, and surface motion due to density jump at the phase transition. Such approach enables us to determine the interface position more precisely. The surface analysis by low-energy-electron diffraction (LEED) indicates that the crystalline structure of the irradiated surface is correlated with the nonequilibrium character of the laser-induced thermal processes described by the theoretical model.

## MATHEMATICAL FORMULATION

The surface of monocrystalline Si is irradiated by ArF excimer laser pulse with energy density  $E$ . Initially, the sample occupies the one-dimensional domain  $\Omega^0 = \langle 0, D \rangle$ , divided into two subdomains  $\Omega_L^0 = \langle 0, Z(0) \rangle$ ,  $\Omega_S^0 = \langle Z(0), D \rangle$ , where  $\Omega_L, \Omega_S$  refer to the liquid and solid phases, respectively,  $Z(0)$  is the position of the phase interface at time  $t = 0$ .

The sample surface moves due to the thermal expansion and different den-

sities of the solid and liquid phases. Then, the subdomains have the form :  $\Omega_L(t) = \langle Z_0(t), Z(t) \rangle$ ,  $\Omega_S(t) = \langle Z(t), D \rangle$  where  $Z_0(t)$  is the position of the sample surface at time  $t$ .

The solution to this problem including the density and volume changes requires solving the three equations representing mass, momentum and energy balances with temperature  $T$ , velocity  $v$  and pressure  $p$  (or normal stress  $\sigma$ ) as unknowns.

The solution can be simplified by several additional assumptions :

- a) the influence of pressure or normal stress on the volume changes is negligible in comparison with the temperature influence
- b) the local time variations of both the kinetic and potential energies are much smaller than the variation of internal energy
- c) the influence of  $p$  or  $\sigma$  on the energy balance is negligible
- d) the internal energy density is a function of temperature only

Under these assumptions we take only mass and internal-energy balances into account, and consider only two variables -  $v$  and  $T$ .

The mass balance of a one-component system can be expressed in the case of the one-dimensional mass transfer as follows :

$$\frac{\partial(\rho v)}{\partial x} = -\frac{\partial \rho}{\partial t} \quad (1)$$

where  $\rho$  is the density and  $v$  is the velocity.

Supposing that

$$\rho = \rho_0(1 - \beta(T - T_r)) \quad (2)$$

where  $\beta$  is the volume thermal expansion coefficient,  $T_r$  is a reference temperature and  $\rho_0$  the density at  $T = T_r$ , we obtain

$$\frac{\partial(\rho v)}{\partial x} = \rho_0 \beta \frac{\partial T}{\partial t} \quad (3)$$

The internal energy balance has the following form

$$\rho c \left( \frac{\partial T}{\partial t} + v \frac{\partial T}{\partial x} \right) = \frac{\partial}{\partial x} \left( k \frac{\partial T}{\partial x} \right) \quad (4)$$

where  $c$  is the specific heat,  $k$  is the thermal conductivity.

Then, considering also a volume source of energy, we obtain a set of equations :

$$\frac{\partial(\rho_i v_i)}{\partial x} = \rho_{i0} \beta_i \frac{\partial T_i}{\partial t} \quad , i = L, S \quad (5)$$

$$\rho_i c_i \left( \frac{\partial T_i}{\partial t} + v_i \frac{\partial T_i}{\partial x} \right) = \frac{\partial}{\partial x} \left( k_i \frac{\partial T_i}{\partial x} \right) + S_i(x, t) \quad , i = L, S \quad (6)$$

where indices  $L, S$  denote the liquid and solid phases, respectively. Conditions at the phase interface  $x = Z(t)$  are described by:

$$\dot{Z} = f(T_z) \quad (7)$$

$$(\rho_S - \rho_L)\dot{Z} = \rho_S v_S - \rho_L v_L \quad (8)$$

$$[\rho_S L(T_z) + (\rho_L c_L - \rho_S c_S)T_z]\dot{Z} = (\rho_L c_L v_L - \rho_S c_S v_S)T_z + k_S \frac{\partial T}{\partial x} - k_L \frac{\partial T}{\partial x} \quad (9)$$

Other boundary and initial conditions are (the initial state being solid) :

$$v_S(D, t) = 0 \quad (10)$$

$$T_S(D, t) = T_0 \quad (11)$$

$$\frac{\partial T_L}{\partial x}(Z_0, t) = 0 \quad (12)$$

$$T_{L,S}(x, 0) = T_0 \quad (13)$$

$$Z(0) = 0 \quad (14)$$

$$Z_0(0) = 0 \quad (15)$$

where  $T_z = T(Z, t)$  denotes the interface temperature. The source term  $S(x, t)$  originating from laser pulse absorption is considered in the form

$$S(x, t) = (1 - R)\alpha I_0(t) \exp[-\alpha(x - Z_0(t))] \quad (16)$$

where  $R$  denotes the reflectivity and  $\alpha$  the optical absorption coefficient. The function  $f(T_z)$  from the relation (7) can be expressed, in accordance to Jackson and Chalmers(1956), as follows :

$$f(T_z) = C_1 \exp(-Q/k_B T_z) (1 - \exp[-L_p(1/T_z - 1/T_{eq})/k_B]) \quad (17)$$

where  $Q$  denotes the activation energy for self-diffusion in the liquid,  $L_p$  is the latent heat of fusion per particle,  $C_1$  is the material constant. The latent heat in the equation (9) must depend on  $T_z$  to assure conservation of energy

$$L(T_z) = L_{eq} + (T_z - T_{eq})(c_L - c_S) \quad (18)$$

where  $L_{eq}$  is the latent heat at the equilibrium phase-transition temperature  $T_{eq}$ .

## NUMERICAL SOLUTION

We employ Galerkin-type finite element method with space and time discretization to solve the system (5)-(15). The problem is twice nonlinear. The first (internal) nonlinearity comes from the character of the algebraic-equation set and the second (external) from conditions at the solid-liquid interface. Therefore, two nested iteration procedures must be used to solve this problem. For both iterations we used the method of successive approximations.

## COMPUTATIONS

Temperature- and velocity fields, time dependences of the liquid-solid- interface position, melting- and solidification velocities and surface position were computed in the dependence on initial sample temperature and laser pulse energy density.

Thermodynamical and optical parameters of the c-Si and l-Si were taken from the following sources :

- a) Desai(1986) :  $T_{eq}, L(T_{eq}), c_S(T), c_L$
- b) Unamuno and Fogarassy(1989) :  $\rho_{0S}, \rho_{0L}$  and all the optical parameters of c-Si and l-Si for ArF excimer laser
- c) Glassbrenner and Slack(1964) :  $k_S(T)$
- d) Wood and Jellison(1984) :  $k_L(T)$
- e) Landolt and Bornstein(1982) :  $\beta_S(T)$
- f) Kluge and Ray(1989) : all the parameters of the function  $\dot{Z} = f(T_z)$  (relation (17) ).

Because of the lack of experimental data for  $\beta_L$ ; we adopted the value  $\beta_L = \beta_S(1600K) = 1.24 \times 10^{-5} K^{-1}$ . In any event, additional numerical tests proved the influence of  $\beta_L$  on the accuracy of temperature- and velocity values to be negligible in comparison with the effect of density changes at the phase transformation.

## EXPERIMENTAL

Samples cut from 0.35 mm thick wafers of the Czochralski-grown, p-type, Si(100) single crystal (5–12  $\Omega$ cm), were irradiated by the ArF ( $\lambda = 193$  nm) excimer laser LAMBDA EMG 100 emitting 10 ns (FWHM) pulses with nearly triangular time shape. Maximum output energy measured by a PHOTON CONTROL thermopile joulemeter was approx. 60 mJ; energy density on the sample surface was controlled by focusing the beam with the help of a fused silica lens ( $f=180$  mm) moved by a micropositioner. Typical dimensions of the laser spot on the sample were approx.  $1-2 \times 2-4$  mm<sup>2</sup>. The study of the irradiated surface structure by low-energy-electron diffraction (LEED) was performed "in situ" in the UHV chamber of a VG ADES 400 photoelectron spectrometer equipped with the Auger electron spectroscopy facility. A basic pressure in the chamber was lower than  $1 \times 10^{-8}$  Pa. The laser beam was directed into the UHV chamber through a fused silica window. A chemical composition of the irradiated surface (contamination) were monitored by "in situ" Auger measurements.

## RESULTS AND DISCUSSION

Fig. 1 shows the LEED pattern intensity profiles (59eV) of the atomically clean surface obtained in UHV by laser pulses with energy density varied from  $0.4 \text{ Jcm}^{-2}$  (melting threshold) to  $0.9 \text{ Jcm}^{-2}$  at constant temperature of the sample  $T_0=300 \text{ K}$  (room temperature-RT). At all energy densities, the LEED patterns displayed the features corresponding to two-domain  $(2 \times 1)\text{Si}(100)$  surface reconstruction. The same surface reconstruction usually results from the cleaning-by-heating procedure commonly used in surface physics. The only difference is in the sharpness of the diffraction spots. In the case of the "heat-cleaned" surface, ordinary as well as extra spots are sharp in contrary to the "laser" surface, where the half-order extra spots are very wide and diffuse. This reflects the smaller size and slight misorientation of the particular domains.

The surface irradiated by the laser pulse with  $E = 0.9 \text{ Jcm}^{-2}$  at sample temperature  $77 \text{ K}$  (liquid nitrogen-LN) exhibits LEED pattern corresponding to "bulklike"  $(1 \times 1) \text{Si}(100)$  structure illustrated by intensity profiles in fig. 2. The careful analysis of diffraction pictures in the wide range of primary beam energies, including background between the spots and spots profiles, shows that  $(1 \times 1)$  structure is only virtual. At certain primary beam energies, the spots split into pairs and, at higher energies, very weak and broad half-order spots (corresponding to  $(2 \times 1)$  reconstruction) were observed. The splitting of the spots and existence or absence of reflections give the evidence about the preferential ordering on the surface and about the dramatic changes in the domains size with  $(2 \times 1)$  reconstruction. For the "heat-cleaned" surface, the sizes of two perpendicular domains are about  $20 \text{ nm}$ , whereas they decrease below  $3.5 \text{ nm}$  after the laser irradiation at LN temperature [Chabal et al. (1981)]. The intensity profiles of the  $(1 \times 1)$  spots at LN temperature differ also strongly from RT ones, reflecting also changes in the underlying atomic layers.

If the initial temperature of the sample is above  $680 \text{ K}$ , the laser irradiation gives rise to the "heat-cleaned"-like  $(2 \times 1)$  structure.

These variations of surface structure can be correlated with our theoretical model of the thermodynamical processes during the resolidification of the melted layer. Figs. 3-4 show calculated velocity of the interface between solid and liquid phases and undercooling of Si melted layer for  $E$  in the range  $0.4$ - $1.2 \text{ Jcm}^{-2}$  at the constant temperature of the irradiated sample  $T_0=300 \text{ K}$ . Figs. 5-8 display the same quantities at constant  $E=0.4 \text{ Jcm}^{-2}$ ,  $E=0.9 \text{ Jcm}^{-2}$  and  $T_0$  varying in the range  $4$ - $1000 \text{ K}$ . The solidification velocity increases relatively fast with decreasing temperature  $T_0$  (see Figs. 5,7). In the considered interval of  $T_0$  the differences between the maximum velocity of the

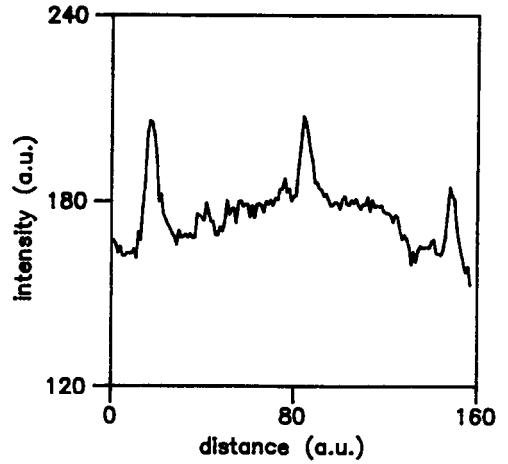
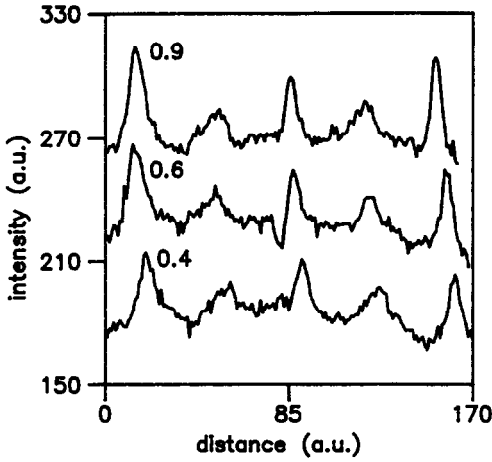


Fig. 1. LEED intensity profiles of surface irradiated by laser pulses with  $E$  from 0.4 to 0.9  $\text{Jcm}^{-2}$  at  $T_0=300$  K.

Fig. 2. LEED intensity profiles of surface irradiated with  $E=0.9$   $\text{Jcm}^{-2}$  at  $T_0=77$  K.

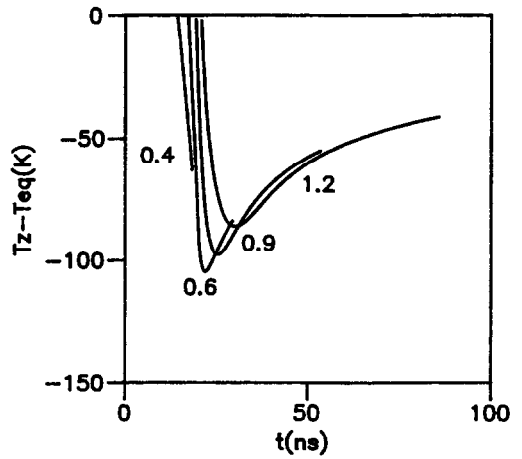
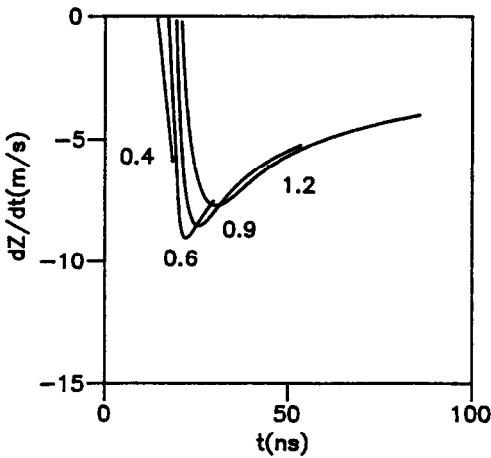


Fig. 3. Phase-interface velocity vs. time for  $E$  from 0.4 to 1.2  $\text{Jcm}^{-2}$  at  $T_0=300$  K.

Fig. 4. Phase-interface undercooling vs. time for  $E$  from 0.4 to 1.2  $\text{Jcm}^{-2}$  at  $T_0=300$  K.

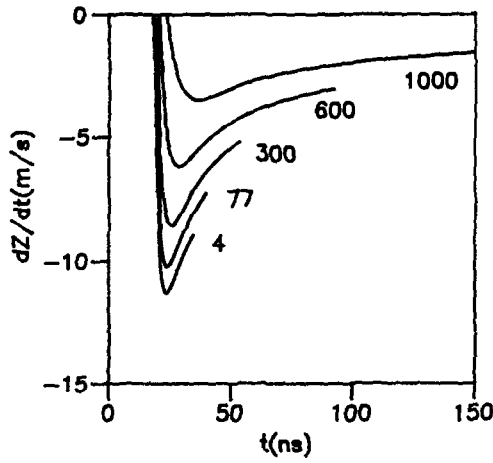


Fig. 5. Phase-interface velocity vs. time for  $T_0$  from 4 to 1000 K at  $E=0.9 \text{ Jcm}^{-2}$ .

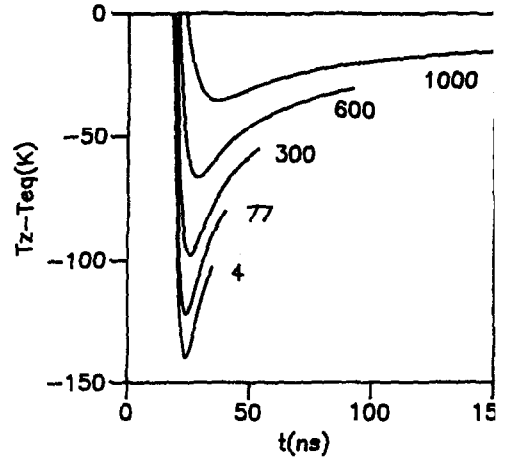


Fig. 6. Phase-interface undercooling vs. time for  $T_0$  from 4 to 1000 K at  $E=0.9 \text{ Jcm}^{-2}$ .

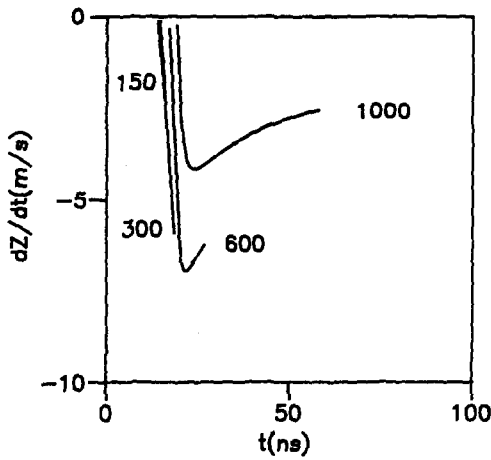


Fig. 7. Phase-interface velocity vs. time for  $T_0$  from 150 to 1000 K at  $E=0.4 \text{ Jcm}^{-2}$ .

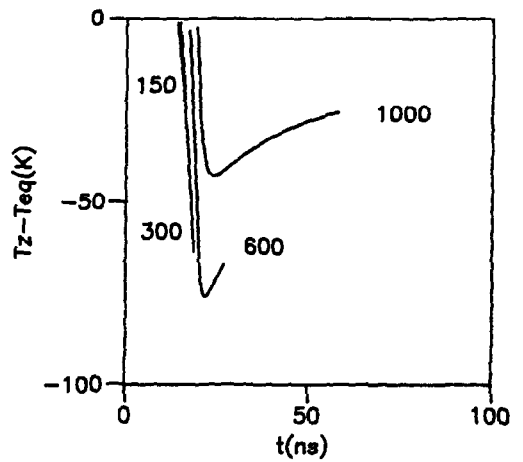


Fig. 8. Phase-interface undercooling vs. time for  $T_0$  from 150 to 1000 K at  $E=0.4 \text{ Jcm}^{-2}$ .



interface motion and the velocity at the moment of complete resolidification are  $\simeq 10 \text{ ms}^{-1}$  and  $\simeq 8 \text{ ms}^{-1}$ , resp. The dependence of interface velocity on the laser-pulse-energy density  $E$  at  $T_0$  fixed is much weaker than that on sample temperature (figs. 3,5). Similarly, the undercooling temperature does not differ too much in the investigated range of energy densities  $E$  (fig. 4) at constant initial sample temperature.

LEED measurements on the laser-irradiated Si(100) surface show a wide variety of surface modifications depending on the pulse energy density and the sample temperature. At the highest energy densities and temperatures, the resulting structure does not differ too much from that obtained by conventional heating procedure. The thermodynamical parameters are similar to those under equilibrium conditions, thus providing the opportunity for the domains to develop the perpendicular orientation of bimer chains. As the solidification time is too short, the domains are slightly misoriented but they are developed enough to be seen by LEED.

On the other side, at low energy densities and temperatures below RT, the thermodynamical conditions are far from equilibrium, thus resulting in deep undercooling of melted silicon and/or different slope of interface velocity (the acceleration of the interface is very high at the moment the solidification is completed). The surface structure is now transformed into the step-like surface with preferential orientation and regular arrangement of the steps. The size of the steps in direction perpendicular to the surface is too small in comparison with the coherence length of LEED. Therefore, this method gives no information about the dimers on the terraces of the steps. By lowering the initial sample temperature, similar effect was observed even at pulse energy densities well above the melting threshold. It should be noticed, that after laser irradiation the sample approaches its initial temperature in the time several orders of magnitude shorter than in the case of usual thermal annealing. Therefore, all the structural effects are predominantly driven by nonequilibrium processes which are expressed by undercooling of melted Si layer and high velocity of the interface between the solid and liquid phases.

## REFERENCES

1. Baeri, P., Campisano, S.U., Foti, G. and Rimini, E., 1979. Melting Model for Pulsing-Laser Annealing of Implanted Semiconductors. *J. Appl. Phys.*, 50: 788-797.
2. Cerny, R., Sasik, R., Lukes, I. and Chab, V., 1991. Excimer-Laser-Induced Melting and Solidification of Monocrystalline Si: The Equilibrium and the Nonequilibrium Models. *Phys. Rev. B*, 44: 4097-4102.
3. Chabal, Y.J., Rowe, J.E. and Christman, S.B., 1981. Nature of Vicinal Laser-Annealed Si(111) Surfaces. *Phys. Rev. B*, 24: 3303-3309.
4. Cullis, A.G., Weber, H.C., Chew, N.G., Poate, J.M. and Baeri, P., 1982. Transitions to

Defective Crystal and the Amorphous State Induced in Elemental Si by Laser Quenching. *Phys. Rev. Lett.*, 49: 219-222.

5. Desai, P.D., 1986. Thermodynamic Properties of Iron and Silicon. *J. Phys. Chem. Ref. Data*, 15: 967-983.
6. Glassbrenner and C.J., Slack, G.A., 1964. Thermal Conductivity of Silicon and Germanium from 3 degrees K to melting point. *Phys. Rev.* 134: A1058-1069.
7. Jackson, K.A. and Chalmers, B., 1956. Kinetics of Solidification. *Can. J. Phys.*, 34: 473-490.
8. Jackson, K.A., 1975. Theory of Melt Growth. In: R. Ueda and J.B. Mullin (Editors), *Crystal Growth and Characterization*. North Holland, Amsterdam, pp. 21-32.
9. Jellison, G.E., Jr., 1984. Optical and Electrical Properties of Pulsed Laser-Annealed Silicon. In: R.F. Wood, C.W. White and R.T. Young (Editors), *Pulsed Laser Processing of Semiconductors, Semiconductors and Semimetals Vol.23*. Academic Press, Orlando, pp. 94-164.
10. Kluge, M.D. and Ray, J.R., 1989. Velocity versus Temperature Relation for Solidification and Melting of Silicon: A Molecular-Dynamics Study. *Phys. Rev. B*, 39: 1738-1746.
11. Kubatova, J., Chab, V., Lukes, I., Jiricek, P. and Fendrych, F., 1989. ArF Excimer Laser Induced Changes in the Si(100)/SiO<sub>2</sub> Interface Studied in Situ by ESCA and LEED. *Appl. Surf. Sci.*, 43: 297-300.
12. Landolt, H and Bornstein, R., 1982. *Numerical Data and Functional Relationships in Science and Technology*, Vol.17, Springer, Berlin.
13. Liu, P.L., Yen, R., Bloembergen, N. and Hodgson, R.T., 1979. Picosecond Laser-Induced Melting and resolidification Morphology on Si. *Appl. Phys. Lett.*, 34: 864-866.
14. Sasik, R. and Cerny, R., 1991. Numerical Solution of the Non-Isothermal Moving Boundary Problem in Heat Conduction. *Comp. Phys. Comm.*, 64: 241-251.
15. Spaepen, F. and Turnbull, D., 1982. Crystallization Processes. In: J.M. Poate and J.W. Mayer (Editors), *Laser Annealing of Semiconductors*. Academic Press, New York, pp. 15-42.
16. Tam, A.C. and Leung, W.P., 1984. Optical Generation and Detection of Acoustic Pulse Profiles in Gases for Novel Ultrasonic-Absorption Spectroscopy. *Phys. Rev. Lett.*, 53: 560-563.
17. Turnbull, D., 1956. Phase Changes. *Sol. State Phys.*, 3: 225-306.
18. De Unamuno, S. and Fogarassy, E., 1989. A Thermal Description of the Melting of c- and a- Silicon under Pulsed Excimer Lasers. *Appl. Surf. Sci.*, 36: 1-11.
19. Wood, R.F. and Jellison, G.E., Jr., 1984. Melting Model of Pulsed Laser Processing. In: R.F. Wood, C.W. White and R.T. Young (Editors), *Pulsed Laser Processing of Semiconductors, Semiconductors and Semimetals Vol.23*. Academic Press, Orlando, pp. 165-250.
20. Wood, R.F. and Geist, G.A., 1986. Modeling of Nonequilibrium Melting and Solidification in Laser-Irradiated Materials. *Phys. Rev. B*, 34: 2606-2620.
21. Wood, R.F. and Giles, G.E., 1981. Macroscopic Theory of Pulsed-Laser Annealing 1. Thermal Transport and Melting. *Phys. Rev. B*, 23: 2923-2942.
22. Zehner, D.M., 1984. Surface Studies of Pulsed Laser Irradiated Semiconductors. In: R.F. Wood, C.W. White and R.T. Young (Editors), *Pulsed Laser Processing of Semiconductors, Semiconductors and Semimetals, Vol.23*. Academic Press, Orlando, pp. 405-470.